Some aspects of offshore pipeline design against upheaval buckling

Rabindra Subedi, Bipul Hawlader & Ashutosh Dhar
Faculty of Engineering and Applied Science
Memorial University of Newfoundland, St. John's, NL, Canada

ABSTRACT
Pipelines are often used to transport hydrocarbon in onshore and offshore environments. In offshore, proper trenching and back-filling are difficult. Therefore, an offshore pipeline might experience both lateral and upheaval buckling during operation at high temperature and high pressure (HT/HP), depending upon the soil resistance. The initial imperfection is another factor that governs the initiation and type of buckling. The existing theoretical solutions have some limitations in modelling initial imperfection and soil resistances. Finite element (FE) simulation is performed for varying initial imperfection and nonlinear soil resistances to investigate the structural response of the pipeline. The effects of burial depth, pipe diameter and wall thickness on operating temperature are studied. The post-peak degradation of uplift resistance plays a significant role in post-buckling behaviour.

RÉSUMÉ
Les pipelines sont souvent utilisés pour transporter des hydrocarbures dans des environnements onshore et offshore. En offshore, il est difficile de creuser des tranchées et de remblayer. Par conséquent, un pipeline offshore peut subir un flambage latéral et bouleversant lors de son fonctionnement à haute température et haute pression (HT/HP), en fonction de la résistance du sol. L'imperfection initiale est un autre facteur qui gouverne l'initiation et le type de flambement. Les solutions théoriques existantes présentent certaines limites pour la modélisation des imperfections initiales et des résistances du sol. En effectuant des simulations par éléments finis (FE) pour faire varier les imperfections initiales et les résistances non linéaires du sol, la réponse structurelle du pipeline est étudiée. Les effets de la profondeur d'enfouissement, du diamètre de la conduite et de l'épaisseur de la paroi sur la température de fonctionnement sont étudiés. La dégradation post-pic de la résistance au soulèvement joue un rôle important dans le comportement après le flambement.

1 INTRODUCTION

Global buckling is one of the major issues in the design of pipeline in offshore environments. The initial out-of-straightness or crookedness which is known as imperfection in a pipeline. The imperfect pipelines might buckle during operation at high temperature and pressure flow of hydrocarbon. In shallow water depths, the pipelines are buried through trenching and backfilling. The burial provides flow assurance and prevents movement of the pipeline during operation. As the lateral resistance is higher, the buried pipeline are typically more susceptible to upheaval buckling (UHB), where the pipeline might move vertically in the upward direction. If an upheaval buckling occurs, the pipeline might come out of the seabed, which creates additional design issues, such as the damage by fishing gears, dropped object and submarine debris flow impact on the suspended section of pipeline. Nielson et al. (1990) reported upheaval buckling at 26 locations of a buried pipeline in the Danish sector of the North Sea. In one segment, a 10-m section moved 1.1 m above the seabed, although the structural failure of the pipeline did not occur.

Offshore pipelines operate at the high-temperature of more than 100 °C and the maximum pressure of around 35 MPa (Hooper et al. 2004). The high temperature and pressure generate axial compressive stress, which could result in the upheaval buckling of the pipeline. Hobbs (1984) used the concept of Tvergaard and Needleman (1981) to develop analytical solutions for upheaval and lateral buckling of submarine pipelines. Nielsen et al. (1988) established a new design procedure for the uplift resistance to control the upward movement of the imperfect pipe below the critical values to avoid progressive upheaval buckling. Palmer et al. (1990) developed a semi-empirical simplified solution for the preliminary design of submarine pipelines against upheaval buckling. Taylor and Gan (1986), and Taylor and Tran (1994) proposed the empathetic, isoprop and blister imperfection models for the submarine pipeline, and theoretically and experimentally analyzed the vertical and lateral buckling. Previous studies like Bransby et al. (2002), Palmer and King (2004), Cheuk (2005) conducted physical modeling for assessment of uplift resistance of buried pipelines. Some studies recognized the effect of post-peak degradation of uplift resistance on UHB (Klever et al. 1990; Goplen et al. 2005; Wang et al. 2009; Thusyanthan et al. 2010). Roy et al. (2018) conducted a numerical analysis to show the importance of post-peak softening in dense sand.

Albeit experimental evidence shows that both the loose and dense sands exhibit a post-peak degradation of uplift resistance, the current design guidelines, such as ALA (2005) uses a bi-linear and DNV (2007) uses a tri-linear force-displacement model for uplift resistance without considering post-peak degradation. The study aims to present finite element (FE) analyses of upheaval buckling of buried offshore pipelines in the sand. The effects of

degradation of post-peak uplift resistance and other parameters are examined. The initiation of buckling and post-buckling behaviour are studied from buckled configuration and plastic strain generation in the pipe.

2 PIPELINE IMPERFECTION

A proper representation of initial imperfection is necessary for modelling UHB. A simple mathematical function may not always represent the actual shape of the imperfect pipe. For example, Mandal and Dhar (2017) compiled the information of a seabed profile and showed that the vertical alignment of the pipe is rather complex. Based on physical imperfection and mathematical reasoning, several methods have been proposed to define the initial imperfection in buckling analysis, which includes isoprop and blister model, empathetic and sinusoidal model, and pipeline weight dependent shape (Taylor and Tran 1996; Palmer and King 2004; Karampour et al. 2013).

In the present study, the initial imperfection, as an empathetic shape (Eq. (1)), is used for numerical analysis (Taylor and Tran 1994)

$$v_o = v_{om}\left\{0.707 - 0.262\pi^2\frac{x^2}{L_o^2} + 0.293\cos\left(2.86\frac{\pi x}{L_o}\right)\right\} \quad [1]$$

where v_o and v_{om} represent the imperfection (vertical distance from the datum to the pipe center) at any point and at the midpoint (x = 0), respectively. The imperfection ratio, $\tilde{v}_{om}(= v_{om}/L_o)$, plays a significant role in UHB, which are related as (Taylor and Gan 1986):

$$\frac{v_{om}}{L_0^4} = 2.407\times10^{-3}\frac{q}{EI} \quad [2]$$

where q is the submerged self-weight of pipe per unit length; EI is the flexural rigidity of the pipe.

3 NUMERICAL MODELLING AND VERIFICATION

The FE model is verified first by comparing the results with the analytical solution developed by Taylor and Gan (1986). They considered the axial resistance per unit length of the pipeline (F_a) as a function of axial displacement (u).

$$F_a = q\phi_a\left(1 - \exp\left(-25u/u_\phi\right)\right) \quad [3]$$

The value of ϕ_a = 0.7 and u_ϕ = 5 mm have been suggested to use by ALA (2005). The pipeline has been assumed to be on a rigid seabed.

In the present FE analysis, the pipeline is idealized as one-dimensional beam elements supported by the axial and vertical downward nonlinear soil springs (Fig. 1). For this analysis, the axial spring has been defined using Eq. (3). A large value of spring constant has been used for the vertical downward spring to simulate a rigid seabed similar to the work of Taylor and Gan (1986) where the upward resistance is zero.

FE analyses are performed using Abaqus/Standard FE software (2014). The modified static RIKS method in the software is used to avoid numerical issues related to unstable buckling behaviour during snap-through buckling, as discussed in the following sections.

For the verification of FE model, a pipeline of 0.65-m outer diameter with a wall thickness of 15 mm having submerged self-weight of 3.8 kN/m is considered. Modelling is performed for a 3,500-m long pipeline section to eliminate the boundary effects on buckling that occurs at the middle of the pipeline. An initial imperfection is provided at the central portion of the pipeline using Eq. (1). The pipeline is discretized using B21H elements, which are a 2-node linear beam in a plane with the hybrid formulation. A mesh sensitivity analysis is performed for varying element length of (0.1 m– 1.0 m); however, no significant change in buckling is found for element size less than 1.0 m. Therefore, all the analyses are performed using 1.0-m long beam elements.

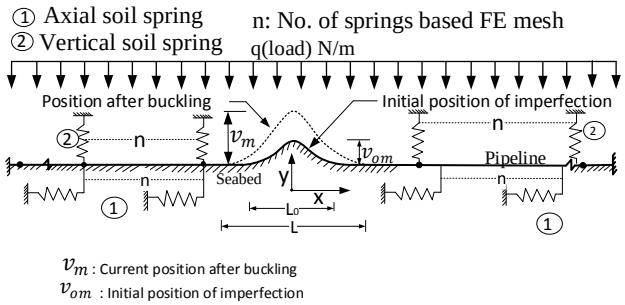

Figure 1. Problem statement and finite element modeling

The soil is modelled using nonlinear springs (SPRING1 in the software) by providing the force–displacement curves as the input for the axial and bearing resistances. The FE analysis consists of two steps: (i) the general static steps for the submerged self-weight of the pipeline was applied as a line load; and (ii) the static RIKS step where the modified RIKS algorithm is used. Also, the temperature is defined in the predefined fields in the ABAQUS for RIKS step. The geometric nonlinearity is considered in both steps. The pipe is modelled as an elastoplastic material.

A fixed boundary condition is applied at the end of the pipe. The numerical simulations are performed for three initial imperfection ratios, $\tilde{v}_{om} = v_{om}/L_o$, of 0.003, 0.007 and 0.010. The FE calculated buckle amplitude (v_m) with pipe temperature (T) is shown in Fig. 2. The dashed lines in Fig. 2 shows the T– v_m curves obtained from theoretical solution (Taylor and Gan 1986). As the same pipe–soil interaction properties (spring constants in FE) are used, the FE calculated curves match well with the theoretical solution. This also implies that the developed FE model can capture snap-through and stable bucking properly. Figure 2 also shows the results obtained from Hobbs (1984), which has been developed for a perfect pipeline (i.e., no initial imperfection).

Figure 2 shows an unstable buckling for a small initial imperfection of 0.003, whereas buckling is stable for higher values of initial imperfection ratio. The critical temperature (T_{cr}) is the maximum temperature before going to the unstable buckle for a small imperfection whereas, for the

higher imperfections, it is the point of intersection of two tangents drawn from the initial and final slopes from stable buckling profile Arman et al. (2017). The safe temperature for buckling is the lowest temperature in a snap through behaviour, whereas it is beyond the point of tangency in stable buckling such that the yield stress does not exceed.

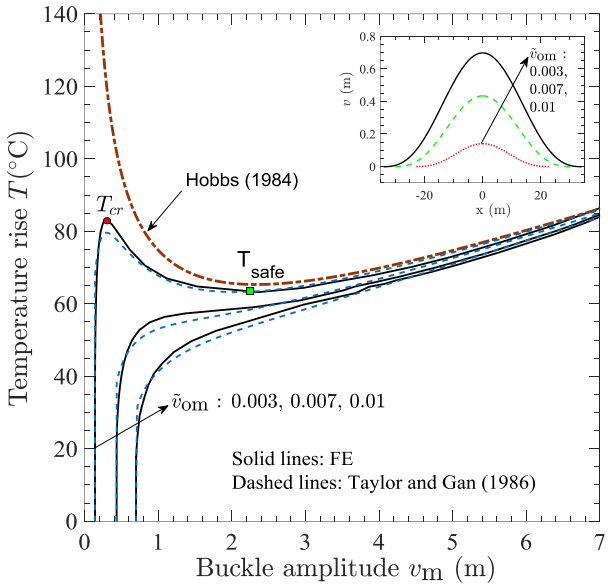

Figure 2. Comparison of FE analysis results with theoretical solutions

4 SOIL RESISTANCE IN DESIGN GUIDELINE

ALA (2005) and DNV (2007) are the two widely used guidelines for pipeline design. In ALA, bi-linear curves are used to define the force–displacement behaviour using soil springs for axial, lateral and vertical directions for a 3D pipeline. Based on ALA (2005), the spring force increases linearly with relative displacement up to the maximum value and then remains constant.

The maximum axial soil resistance per unit length of the pipeline (F_{ap}) buried in sand can be calculated as:

$$F_{ap} = 0.5\,\pi DH\gamma(1+K_0)\tan\left(\phi_\mu\right) \quad [4]$$

where γ is the effective unit weight of soil; H is the burial depth from the center of the pipe; D is the diameter of the pipe; K_0 is the coefficient of earth pressure at rest; ϕ_μ is the axial interface friction angle between pipe and soil. The burial depth is expressed in a normalized form for using embedment ratio, $\tilde{H}$ (= H/D). ALA (2005) also suggested that the relative axial displacement (u) required to mobilize the peak (u_p) is 3 mm and 5 mm for dense and loose sands, respectively.

The maximum bearing resistance (F_{bp}) for sand can be calculated as (ALA 2005):

$$F_{bp} = N_q\gamma HD + 0.5D^2\gamma N_\gamma D^2 \quad [5]$$

where $N_q = e^{(\pi\tan\phi')}\tan^2(45^\circ+\phi'/2)$, $N_\gamma = e^{(0.18\phi'-2.5)}$ are the bearing capacity factors. Again, the vertical penetration resistance (F_b) increases linearly with downward movement (v_b), at v = v_{bp} it reaches the F_{bp} and then remains constant. Moreover, v_{bp} is related to the diameter of the pipe as v_{bp} = 0.1D, for sand.

The maximum vertical uplift resistance (F_{up}) for the pipeline in sand can be calculated as (ALA 2005):

$$F_{up} = N_{qv}\gamma HD \quad [6]$$

where $N_{qv} = \phi' H/44D$ ($\leq N_q$ in bearing capacity equation (Eq. (5)) and ϕ' is in degree. Again, the upward resistance (F_u) increases linearly with upward displacement (v) and, at $v = v_p$, the maximum resistance F_{up} is mobilized. After v_p, the upward resistance remains constant at F_{up}. ALA (2005) suggested that v_p is related to burial depth (H) as v_p = 0.01H–0.02H for sand.

DNV (2007) suggested a trilinear force–displacement curve for uplift resistance. The peak uplift resistance can be calculated as:

$$F_{up} = \left(1+f\tilde{H}\right)\gamma\tilde{H}D^2 \quad [7]$$

where f is the uplift resistance factor. DNV (2007) suggested f = 0.1–0.3 and f = 0.4–0.6 for loose and medium/dense sands, respectively. The maximum uplift resistance mobilizes at v_p = 0.005H–0.008H, which is lower than the v_p recommended by ALA (2005), as mentioned above.

The force–displacement curve prior to the peak is defined by two linear segments that intersect at a point below the peak (βv_p, αF_{up}, where α and β are two constants). DNV (2007) recommended β = 0.2, and α = 0.75–0.85 and α = 0.65–0.75 for loose and dense sands, respectively. The lower and upper values of f and α represent the lower bound (LB) and upper bound (UB), respectively. The geometry and material properties used in the current analysis is shown in Table 1.

5 LIMITATIONS IN MODELING OF UPLIFT BEHAVIOUR

DNV (2007), ALA (2005) guidelines suggest that the uplift resistance after the peak remains constant. However, the works by Trautmann et al. (1985), Nielsen et al. (1990), Klever et al. (1990), Cheuk (2005), Goplen et al. (2005), Wang et al. (2012) suggest that the soil resistance gradually decreases after the peak for shallow to intermediate burial depths. At a large displacement, the reduction of uplift resistance is significant. Physical experiments show that it becomes zero (as expected) when the pipeline moves to the ground surface (Wang et al. 2012). Observing large upward displacement in the field, Nielsen et al. (1990) schematically show the typical nonlinear uplift resistance curve (solid line in Fig. 3). Three discrete points are used to characterize the force–displacement behavior. The submerged self-weight of the pipe plus the weight of the soil column directly above the

pipe corresponds to point 1 where the upward displacement is assumed to be zero.

From point 1 to 2, the continuous upward movement of the imperfect pipe section mobilizes at an uplift resistance

Table 1. Geometry and material properties used in analysis

Parameters	Value
Length of pipe, L (m)	3500
External diameter of pipe, *D* (mm)	300
Wall thickness of pipe, *t* (mm)	12.7
Thickness of concrete cover (m)	0.05
Density of steel, ρ_s (kg/m^3)	7850
Density of concrete, ρ_c (kg/m^3)	2800
Density of oil, ρ_o (kg/m^3)	800
Submerged weight of oil-filled pipe, *q* (N/m)	1594
Angle of internal friction of soil, ϕ' (°)	35
Coefficient of earth pressure at-rest, K_0	0.5
Effective unit weight of soil, γ (kN/m^3)	9
Axial interface friction angle, ϕ_μ (°)	28
Young's modulus of pipe, *E* (GPa)	206
Poisson's ratio of pipe (ν)	0.3
Yield stress of pipe, σ_y (MPa)	448
Ultimate strength, σ_{ult} (MPa)	531
Coefficient of thermal expansion, α (/°C)	11×10^{-6}

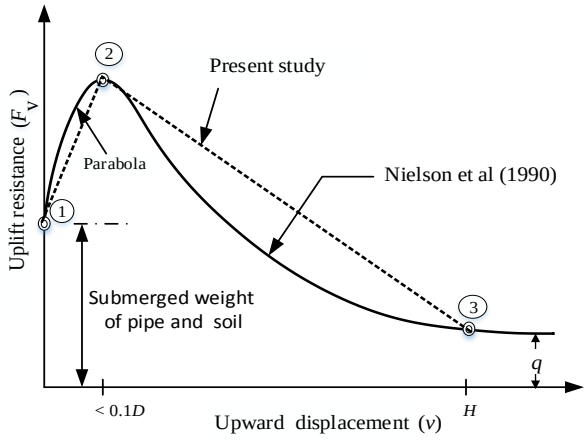

Figure 3. Uplift force–displacement behavior

due to the activation of shear stresses in the soil. Based on physical experimental results (Trautmann et al. 1985), Nielsen et al. (1990) suggested that the displacement required to reach the peak uplift resistance at point 2 is $(0.02 + 0.008H/D)D \leq 0.1D$. Once the upward movement of the pipe exceeds the displacement required to reach the peak uplift resistance, the general shear failure occurs in the soil, resulting in degradation of uplift resistance until the point 3 when the pipe reaches the ground surface or seabed.

Numerical modeling also shows a nonlinear post-peak reduction of uplift resistance, F_v (Roy et al. 2018). For dense sand, F_v reduces quickly immediately after the peak, which is due to the reduction of shear strength parameters (friction and dilation angles) with the development of plastic shear strains. At large displacements, the reduction of F_v mainly occurs due to the reduction of cover depth.

Although the post-peak behaviour is nonlinear, a linear degradation of uplift resistance, as shown by the dashed line in Fig. 3, is used in this study. Note that a linear post-peak degradation model will not be valid for pipelines at large burial depths. Therefore, the analyses are performed for the embedment ratio ($\tilde{H}$) of 1–3. The peak value (F_{up}) is calculated based on ALA (2005) and DNV (2007) (Eqs. 6 and 7). In the calculation with DNV, $\alpha = 0.65$ (LB), $\alpha = 0.75$ (UB), $\beta = 0.2$, $f = 0.4$ (LB) and f = 0.6 (UB) are used. As an example, for the soil parameters listed in Table 1 and $\tilde{H} = 3$, the calculated F_{vp} = 5921 N/m (ALA) and F_{vp} = 5459 N/m (DNV LB) and F_{vp} = 6948 N/m (DNV UB). Note that DNV (2007) somehow recognized the importance of post-peak degradation of uplift resistance, but ALA (2005) is silent on post-peak degradation. In the following sections, where the post-peak degradation is considered, the force–displacement relationship up to the peak is calculated based on DNV (2007) upper or lower bounds.

6 EFFECTS OF AXIAL RESISTANCE IN BUCKLED SECTION

The axial soil resistance has a significant impact on UHB. Theoretically, the axial resistance should be reduced once the pipe buckles upward from the initial position because of reduction of cover depth, and the axial resistance will be zero when it moves above the seabed. However, the variation in axial spring resistance with upward displacement adds additional complexities in numerical simulation using the built-in modelling approaches available in the software. Therefore, to check the effect of this, analyses are performed for the following axial resistances in the central portion ($2L_o$) of the pipeline (Fig. 1) where buckling occurs: (i) full axial resistance using Eq. (4), (ii) no axial resistance, which is a conservative assumption, and (iii) half of the axial resistance based on Eq. (4) (average of the above two). Outside the possible buckled zone, i.e. beyond $2L_o$ length of initial imperfection full axial resistance is used for all three cases.

Figure 4 shows that the variation in axial resistance in the buckled segment (full to zero) does not have a significant effect on the critical temperature. However, the safe temperature decreases considerably—as an example, for the initial imperfection ratio of 0.003 the safe temperature decreases by ~12 °C when zero axial resistance is used instead of full resistance (see the inset of Fig. 4). In the following sections, all the analyses are performed with the full axial resistance.

7 EFFECTS OF INITIAL IMPERFECTION AND EMBEDMENT RATIO

The temperature rise versus maximum buckle amplitude for different initial imperfections and embedment ratios are presented in Fig. 5(a). In these simulations, the peak

resistance is calculated using ALA (2005) and DNV (2007) (Eqs. 4–7), together with the linear decrease in post-peak resistance (Fig. 3) for DNV only. Both critical and safe temperatures increase with embedment ratio (Fig. 5(b)). The critical and safe temperature is higher if the post-peak degradation in uplift resistance is not considered (i.e., soil resistance remains constant after the peak). Due to post-peak degradation, the safe temperature decreases more than the critical temperature, and it is even more significant for larger burial depths.

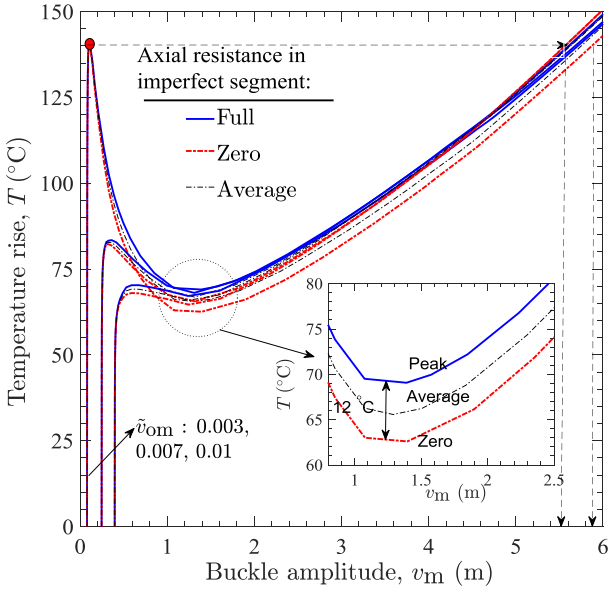

Figure 4. Effects of axial resistance in imperfect section

Similar analyses are performed with DNV (2007) upper bound up to the peak, together with a linear decrease in the post-peak region. The temperature rises with maximum buckle amplitude is shown in Fig. 6. Again, the post-peak degradation in uplift resistance significantly reduces the safe temperature as compared to the critical temperature.

8 VERTICAL DEFORMATION AND PLASTIC SHEAR STRAIN

The selection of maximum buckling temperature and corresponding maximum buckle amplitude for the design of offshore pipeline is challenging. If the design is based on a strain-based design criterion, the pipe might be able to move a sufficiently large vertical distance from the initial position without failure Bai and Bai (2005).

Figure 7(a) shows the vertical displacement of the pipe (including the initial imperfection v_o) along the length from the midpoint for a pipeline of $\tilde{v} = 0.003$ and $\tilde{H} = 3$. The maximum (critical) temperature (T_{cr}) before snap-through is 139 °C, which increases gradually with an increase in vertical displacement. As the maximum buckle amplitude before reaching T_{cr} is small (≤ 0.096 mm), the pipe displacements for this range is shown in the inset of Fig. 7(a). After reaching the critical temperature, the pipe temperature decreases but the vertical displacement continues because of snap-through buckling (see Fig. 6). Figure 6 also shows that, if the operating temperature somehow exceeds the critical temperature, a sudden uplift of 5.8 m occurs, as shown by drawing a horizontal line from T_{cr} to the T–v_m curve in Fig. 6. This could result in movement of a segment of the pipe above the seabed. Nielson et al. (1990) reported a 10-m pipe segment moved above the seabed due to upheaval buckling. The lowest (safe) temperature is 69 °C.

The strain-based criteria are currently used in the design of the pipeline, where the strain is maintained below an allowable strain, typically 1%–2% (Palmer et al. 1990). Figure 7(b) shows the longitudinal plastic strains (ε_p) developed in the pipe. The plastic strains generated at the midsection of the pipe and at the end of the buckled section where the curvature is high (Fig. 7(a)). For this analysis, $\varepsilon_p \geq 0.02$ in the snap-through zone when T ~ 110 °C and the maximum buckle amplitude of 4.2 m.

9 EFFECTS OF PIPE DIAMETER AND WALL THICKNESS

The cross-sectional properties of pipe play an essential role in buckling, which is investigated using varying pipe diameter and wall thickness. Only one parameter is varied in the analysis, while the other parameters are the same as Table 1. The uplift force–displacement behaviour based on DNV LB with post-peak softening (Fig. 3) is considered. Analyses are performed for $\tilde{H}$ = 3, and two imperfection ratios, $\tilde{v}_{0m}$ = 0.003 and 0.01.

9.1 Diameter

Three pipelines of 0.1413-m, 0.2985-m, and 0.4064-m diameter, with the same wall thickness of 0.0127 m, are considered, which covers the commonly used offshore pipeline sizes. The submerged self-weight of the pipeline for the oil-filled condition is calculated as 0.85 kN/m, 1.59 kN/m, 2.05 kN/m, respectively. Figure 8 shows the buckling response for six analyses. As the pipe diameter is different, initial imperfection, including initial buckle amplitude v_{om} is different for a given $\tilde{v}_{0m}$.

Figure 8 shows that the critical and safe buckling temperatures increase with pipe diameter. For example, T_{cr} = 60 °C and 121 °C for 141.3-mm and 298.5 mm diameter pipes, respectively, for the initial imperfection ratio of 0.003.

9.2 Wall Thickness

Four analyses are performed for varying wall thickness, t (= 8.8 mm, 10.3 mm, 12.7 mm, and 14.3 mm) for pipe diameter of 0.3 m. The other parameters are listed in Table 1. The submerged weight of the pipe decreases with a reduction in wall thickness, which lowers the effective axial compression. The numerical analyses show that the thinner pipe wall has higher upheaval buckling resistance than the thicker pipe wall for the same outer diameter (Fig. 9). The critical and safe buckling temperature decreases

with the increase in pipe thickness. Palmer et al. (1990) suggested a reduced wall thickness to minimize potential upheaval buckling.

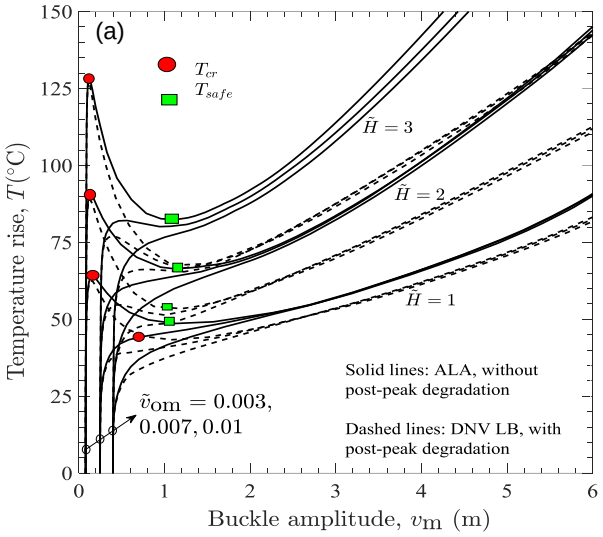

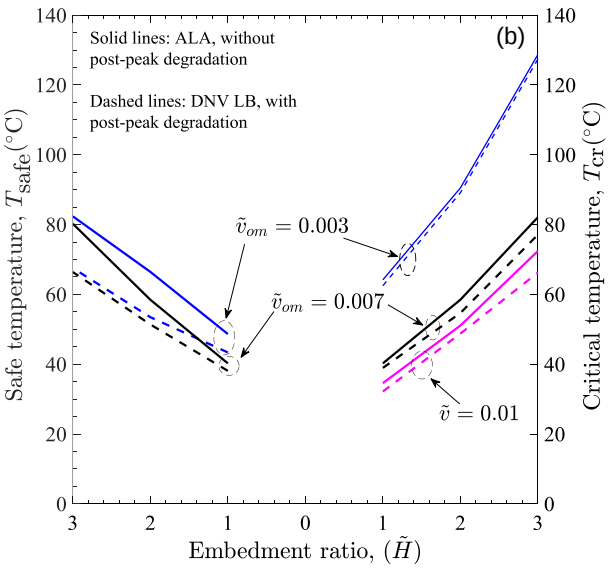

Figure 5. Effects of burial depth: (a) Buckling profile; and (b) Safe and critical temperatures

10 CONCLUSIONS

The aim of the current design guidelines for upheaval buckling is to ensure that the pipeline remains in place during operation (DNV 2007). However, many field observation shows significant upward displacements due to upheaval buckling. The present study examines the response of buried offshore pipelines if upheaval buckling occurs. The upward displacement of the pipe could reduce

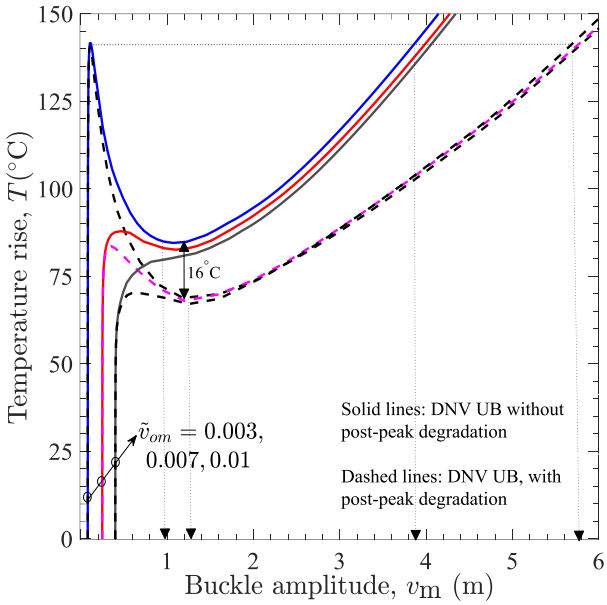

Figure 6. Effects of post-peak softening with DNV UB soil spring properties

the uplift resistance, which is considered in the analysis using a linear post-peak degradation model as a function of upward displacement. It is shown that the pipeline might displace a large vertical distance, even might move above the seabed, especially in snap-through buckling cases. However, the generated plastic strains might be within the allowable limit for this large displacement, and therefore, structural failure may not occur. One of the limitations of this study is that the linear post-peak strength degradation model used in this study is valid for loose to medium sand and the pipelines at shallow burial depths.

11 ACKNOWLEDGEMENTS

The works presented in this paper have been supported by the Research and Development Corporation of Newfoundland and Labrador through the ArcticTECH program and the Natural Sciences and Engineering Research Council of Canada (NSERC).

REFERENCES

Abaqus, V. 2014. 6.14 documentation. Dassault Systemes Simulia Corporation, 651.

ALA 2005. Guidelines for the design of buried steel pipe. In American Society of Civil Engineers.

API Design, C. 1999. Operation and maintenance of offshore hydrocarbon pipelines (limit state design). API recommended Practice, 1111.

Amin Arman, Riyadul & Roy, Kshama & Hawlader, Bipul & Dhar, Ashutosh. 2017. Finite Element Analysis of Upheaval Buckling of Submarine Pipelines with Initial Imperfection.

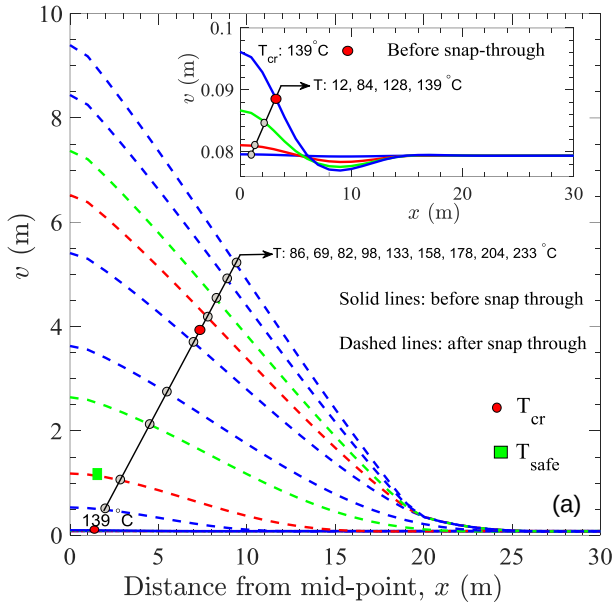

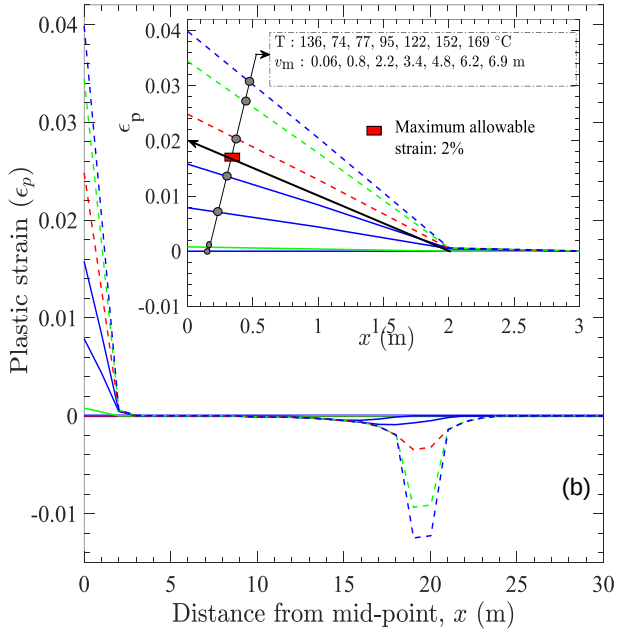

Figure 7. Response to temperature loading: (a) Pipeline profile; and (b) Plastic strain in pipeline

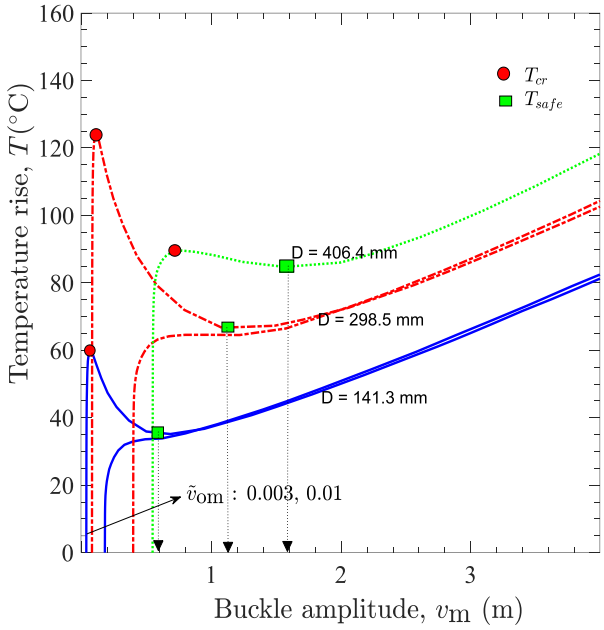

Figure 8. Effects of the pipe diameter

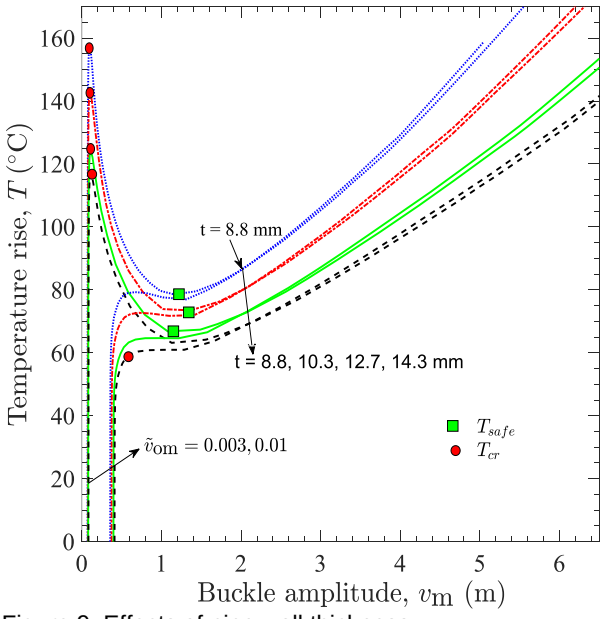

Figure 9. Effects of pipe wall thickness

Bransby, M., Newson, T., and Brunning, P. 2002. The upheaval capacity of pipelines in jetted clay backfill. International Journal of Offshore and Polar Engineering

Cheuk, C. Y. 2005. Soil-pipeline interaction at the seabed. PhD thesis, University of Cambridge, UK.

Crisfield, M. 1981. A fast incremental/iterative solution procedure that handles "snap-through". In Computational Methods in Nonlinear Structural and Solid Mechanics, pages 55–62. Elsevier.

DNV 2007. Global buckling of submarine pipelines–structural design due to high temperature/high pressure. RP-F110, Oslo, Norway.

Goplen, S., Strom, P., Levold, E., and Mork, K. J. 2005. Hotpipe JIP: HP/HT buried pipelines. In ASME 2005 24th International Conference on Offshore Mechanics and Arctic Engineering, pages 691–699. American Society of Mechanical Engineers.

Hobbs, R. E. 1984. In-service buckling of heated pipelines. Journal of Transportation Engineering, 110(2): 175–189.

Hooper, J., Maschner, E., and Farrant, T. 2004. Penguins pipeline system–design challenges for the world's longest snaked lay HP/HT pipe tie-back. In Offshore Pipeline Technology Conference

Karampour, H., Albermani, F., and Gross, J. 2013. On lateral and upheaval buckling of subsea pipelines. Engineering structures, 52:317–330.

Klever, F., Van Helvoirt, L., Sluyterman, A., et al. 1990. A dedicated finite-element model for analyzing upheaval buckling response of submarine pipelines. In Offshore Technology Conference.

Liu, R., Wang, W.G., and Yan, S.W. 2013. Finite element analysis on thermal upheaval buckling of submarine burial pipelines with initial imperfection. Journal of Central South University, 20(1):236–245.

Maltby, T. C. and Calladine, C. R. 1995. An investigation into upheaval buckling of buried pipelines—ii. Theory and analysis of experimental observations. International journal of mechanical sciences, 37(9):965–983.

Mondal, B.C. and Dhar, A.S., 2017. Upheaval buckling of surface-laid offshore pipeline. Applied Ocean Research, 66, pp.146-155.

Nielsen, N., Pedersen, P., Gundby, A., and Lyngberg, B. 1988. Design criteria for upheaval creep of buried subsea pipelines. Offshore Mech Arct Eng ASME, 112:11–22.

Palmer, A., Ellinas, C., Richards, D., Guijt, J., et al. 1990. Design of submarine pipelines against upheaval buckling. Offshore Technology Conference.

Palmer, A. C. and King, R. A. 2004. Subsea pipeline engineering. PennWell Books.

Roy, K., Hawlader, B., Kenny, S., and Moore, I. (2018). Upward pipe–soil interaction for shallowly buried pipelines in dense sand. Journal of Geotechnical and Geo-environmental Engineering, 144(11): 04018078.

Taylor, N. and Gan, A. B. 1986. Submarine pipeline buckling imperfection studies. Thin-Walled Structures, 4(4): 295–323.

Taylor, N. and Tran, V. 1994. Experimental and theoretical studies in subsea pipeline buckling. Marine Structures, 9(2):211–257.

Thusyanthan, N., Mesmar, S., Wang, J., and Haigh, S. 2010. Uplift resistance of buried pipelines and dnv-rp-f110 guidelines. In Proc. Offshore Pipeline and Technology Conference, pages 24– 25.

Tvergaard, V. and Needleman, A. 1981. On localized thermal track buckling. International Journal of Mechanical Sciences, 23(10):577–587.

Wang, J., Eltaher, A., Jukes, P., Sun, J., Wang, F. S., et al. 2009. Latest developments in upheaval buckling analysis for buried pipelines. In the Nineteenth International Offshore and Polar Engineering Conference. International Society of Offshore and Polar Engineers.

Wang, J., Haigh, S., Thusyanthan, N., and Mesmar, S. 2010. Mobilization distance in uplift resistance modeling of pipelines. Proc. International Symposium on Frontiers in Offshore Geotechnics, pages 8–10.

Yong Bai and Qiang Bai 2005. Subsea Pipelines and Risers, Elsevier

Zeng, X., Duan, M., and Che, X. 2014. Critical upheaval buckling forces of imperfect pipelines. Applied Ocean Research, 45:33–39.